Nuclear Instruments and Methods in Physics Research A 646 (2011) 1–6

Contents lists available at ScienceDirect

Nuclear Instruments and Methods in Physics Research A

journal homepage: www.elsevier.com/locate/nima

Lifetime and strength tests of tantalum and tungsten under thermal shock for a Neutrino Factory target

J.R.J. Bennett [a,*], G.P. Škoro [b], John Back [c], S.J. Brooks [a], T.R. Edgecock [a,d], S.A. Gray [a], A.J. McFarland [a], K.J. Rodgers [a], C.N. Booth [b]

[a] STFC, Rutherford Appleton Laboratory, Harwell Science and Innovation Campus, Didcot, OX11 0QX, UK
[b] Department of Physics and Astronomy, University of Sheffield, Sheffield, S3 7RH, UK
[c] Department of Physics, University of Warwick, Coventry, CV4 7AL, UK
[d] University of Huddersfield, Queensgate, Huddersfield, HD1 3DH, UK

ARTICLE INFO

Article history:
Received 7 January 2011
Received in revised form
4 March 2011
Accepted 20 March 2011
Available online 8 April 2011

Keywords:
Tantalum
Tungsten
Thermal shock
Material strength
Target lifetime
Neutrino Factory

ABSTRACT

A description is given of tests on tantalum and tungsten wires to evaluate their lifetime and strength under the thermal shock that will be experienced when a solid target is bombarded with short pulses of high energy protons in a Neutrino Factory. The results of lifetime tests and measurements of dynamic strength characteristics at high temperatures, stresses and strain rates using a laser Doppler vibrometer are given. The tests show that a solid tungsten target will have a life of at least 3 years, which, with other beneficial characteristics, make it an excellent candidate for the Neutrino Factory.

1. Introduction

There are proposals to build a Neutrino Factory [1] to measure the properties of neutrinos. Intense pulsed beams of energetic protons will hit a target to produce pions, which will decay to muons and ultimately to neutrinos. In the current Neutrino Factory baseline design, the proton beam will consist of three micro-pulses each a few nanoseconds long and this macro-pulse is repeated at 50 Hz. The average proton beam power is 4 MW of which $\sim$0.7 MW will be dissipated in the target.

The target sits in a strong solenoidal magnetic field in order to capture and focus the pions emanating from the target in all directions. Maximising the pion yield [2–4] using the MARS code [5] indicates that the proton energy should be in the range 5–10 GeV and that the target should be of a heavy metal with dimensions of $\sim$1 cm in diameter and $\sim$20 cm long. The variation of pion yield with target radius is quite flat and a target of 2 cm diameter, 20 cm long with a proton beam of 2 cm diameter is considered in this paper to reduce the stress and temperature in the target. Initially tantalum was considered a good candidate for the target material due to its high density and known resistance [6] to radiation damage under proton irradiation up to at least 12 dpa on ISIS [7]. However, tantalum becomes too weak at high temperatures [8] and was abandoned in favour of tungsten, which is much stronger [9]. Also, tungsten appears from the experience on ISIS [7] with proton beams up to 12 dpa to have good radiation resistance. Alloys of tungsten, such as tungsten rhenium, are even stronger at high temperatures [9], but alloys generally do not have the same resistance to radiation damage as the pure metals and hence were not considered.

It is extremely difficult to cool a target of these dimensions with a 700 kW load. A free flowing mercury jet has been proposed [10,11], which will readily remove the heat and overcome the problems of thermal shock. This was originally thought to be a serious problem with a solid target due to the high energy density ($\sim$300 J cm^{-3} per macro-pulse) deposited in a very short time. However, King et al. [12] proposed a rotating metal band target, cooled by jets of water, on the basis that the Pbar target [13] at FNAL, used to produce antiprotons for the Tevatron, did not suffer from thermal shock at considerably higher energy densities. Hurh [14] conducted a test on a tantalum disc in the Pbar target, which showed little signs of damage after 1100 pulses at an energy density of nearly 40,000 J cm^{-3}. It is well known that the strength of materials can be enhanced under dynamic conditions [15] and

* Corresponding author. Tel.: +44 1235 446379.
E-mail address: roger.bennett@stfc.ac.uk (J.R.J. Bennett).

0168-9002/$ - see front matter © 2011 Elsevier B.V. All rights reserved.
doi:10.1016/j.nima.2011.03.036

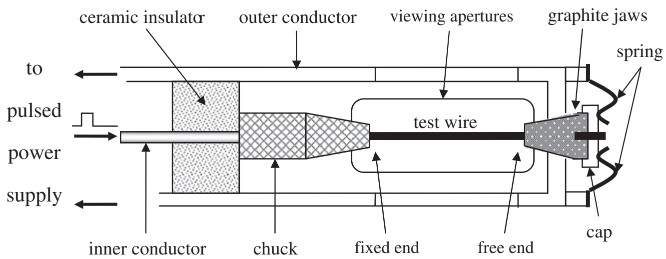

Fig. 1. Schematic diagram of the wire test equipment, showing the chuck clamping one end of the wire and the other end under light spring pressure to allow free axial motion. There are four viewing apertures cut in the outer conductor adjacent to the test wire.

tends to increase at higher strain rates. This is the situation in the Neutrino Factory target, where the thermal shock stress waves have frequencies of the order of 10 kHz.

As a result the proposed solid target for the UK Neutrino Factory is based on bars of refractory metal, which are cooled by thermal radiation at $\sim$1200 °C. About 500 bars, 2 cm diameter and 20 cm long will be required, which will be circulated so that a new bar is presented to each beam macro-pulse every 20 ms.

More recently a flowing tungsten powder target has been proposed [16], which avoids the problems of shock due to the small size of the powder particles.

The problems of thermal shock and lifetime have been addressed in previous papers [17–21], including experiments utilising a fast current pulse through thin wires of tantalum and tungsten. Recent tests [22] using a laser Doppler vibrometer [23] to measure the surface vibrations, have given new results [24] on Young's modulus of elasticity at high strain rates, high temperatures and stress.

In this paper a comparison is made between the measured surface vibrations and simulations using MARS [5] and LS-DYNA [25] codes. In addition to new lifetime measurements, the ultimate yield strength of the material under dynamic test conditions has been measured at high stresses and temperatures. Most measurements at high strain rates use ballistic methods [15], but passing a fast current pulse through a thin wire mimics far more closely the proton beam passing though a target bar.

2. Test equipment

Fig. 1 shows a schematic diagram of the equipment used to shock the wire samples. A straight tantalum or tungsten wire of 0.3–1 mm diameter and 5–10 cm in length is mounted in a small commercial steel chuck, which firmly grips one end of the wire. The other end is free to move axially through four graphite electrodes; if the end was not free the wire would buckle under thermal expansion when heated. Springs apply a light pressure to the graphite, which apply a radial load to the wire through the tapered section. This ensures a reliable electrical connection to the free end of the wire.

The tungsten and tantalum wires were manufactured by standard powder metallurgy methods—pressing, sintering, forging and finally drawing. The wires were $\geq$99.9% pure. The tungsten wires were stress relieved at about 400 °C. All wires were purchased from Goodfellow Cambridge Ltd.[1]

The wire assembly forms the end of a coaxial electrical connection to the pulsed power supply—the spare extraction kicker power supply for the pulsed neutron source, ISIS [7]. The assembly is in a high vacuum (10^{-7}–10^{-6} mbar) to avoid oxidation. A current transformer is used to measure the current pulse on an oscilloscope.

The laser Doppler vibrometer is located outside the vacuum system and can be used to measure the radial or longitudinal vibrations of the wire. An optical pyrometer is used to measure the temperature of the wire at the same point measured by the vibrometer. All observations are made through vacuum windows.

3. Measurement and modelling of stress and surface vibration

The stress in a target is modelled using the MARS code [5] to calculate the energy density deposited in the target by the proton beam as a function of position, and then in-putting this data into the LS-DYNA code [25]. The beam is assumed parabolic in profile, with a diameter equal to that of the target.

The stress has also been modelled for beams that are not coaxial with the target and at an angle to the target axis. In both cases the increase in stress is small; for example, a beam off axis by 0.75 mm to a 1 cm radius target gives a 10% increase in stress.

The first step in modelling the stress in the test wire is to calculate the diffusion of the current into the wire with the application of the fast current pulse. A typical current pulse is shown in Fig. 2; it consists of the main pulse with a rise time of $\sim$100 ns, a flat top of $\sim$800 ns and is followed by a number of smaller pulses. The power supply will deliver up to 8 kA (peak) at up to 50 Hz. The stress in the test wires is modelled as follows: (1) the current pulse in the wire is measured; (2) the current pulse is approximated by exponential and linear waveforms; (3) the current density, j, is calculated as a function of time, t, and radius, r, using the solution to the diffusion equation [26]. (This is a good approximation for tantalum, but a correction must be made for tungsten because of the higher electrical conductivity.); (4) knowing the current density, the temperature rise is calculated as a function of time and radius; (5) LS-DYNA is used to calculate the resultant stress as a function of time and radius.

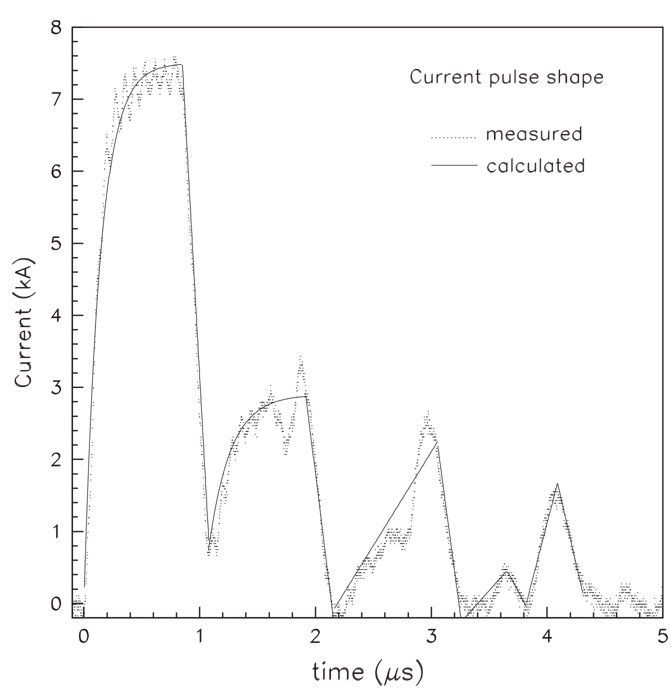

Fig. 2. Measured pulse current from the power supply (dotted line) and the current modelling used in the calculations (solid line).

[1] http://www.goodfellow.com/

In addition to the thermal stress, the Lorenz magnetic force due to the current in the wire, must be added.

The material parameters used in the above calculations are taken from the literature [27,28] and Young's modulus of elasticity from [24]. Fig. 3 shows the resultant calculated stress in a 0.5 mm diameter wire with a 7.2 kA current pulse at a peak temperature of 1260 °C.

A single pulse of protons (repetition rate of 50 Hz) gives a very high stress in the target and it is necessary to have an odd number (3, 5, etc.) of micro-pulses (1–3 ns long) judiciously spaced to minimise the stress. More than one micro-pulse is also necessary

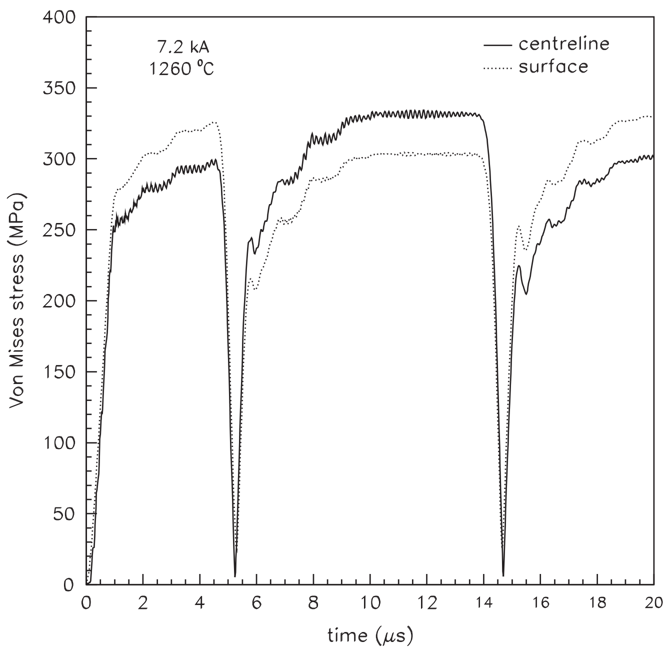

Fig. 3. Calculated stress in the wire with a current pulse of 7.2 kA at a peak temperature of 1260 °C.

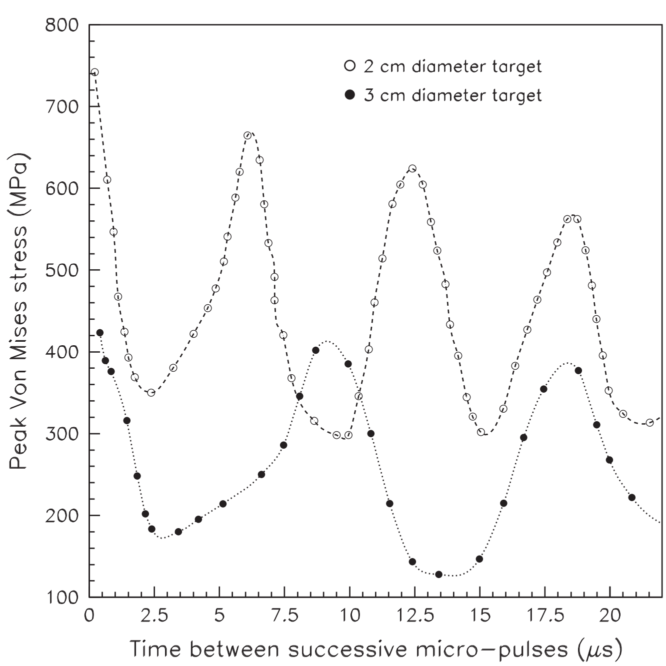

Fig. 4. Peak Von Misses stress as a function of the time between each of three micro-pulses for a target bar of 2 and 3 cm diameter.

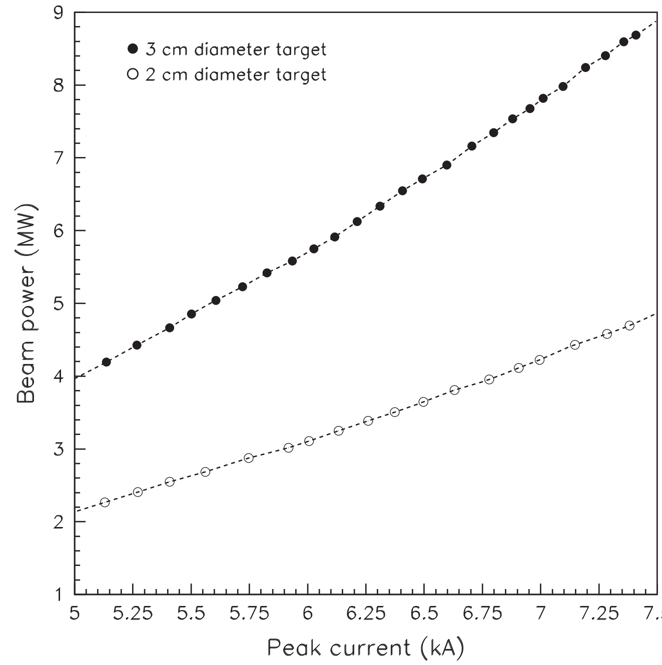

Fig. 5. Pulse current in a 0.5 mm tungsten wire versus the beam power on a target of 2 and 3 cm diameter, which produce the same peak Von Misses stress in both cases.

to keep the short pulse length in the proton accelerator due to the high space charge forces. Three micro-pulses, spaced at ~10 μs, are proposed for each macro-pulse and this scheme is used throughout the paper. Fig. 4 shows the stress as a function of time between each micro-pulse for targets of 2 and 3 cm diameter. More micro-pulses give slightly lower stress.

It is now possible to relate the current in the wire to the equivalent stress in the target. Fig. 5 (taken from Ref. [22]) shows the pulse current required to simulate various beam powers in a target of 2 and 3 cm diameter.

Fig. 6 shows the radial velocity modelled in the wire compared to that measured by the laser Doppler vibrometer at 900, 1260 and 1450 °C. The agreement is very good, particularly when one takes into account the level of noise on the vibrometer measurement (seen before the pulse arrives at $t=0$) and the uncertainties due to possible movements in the fixed end of the wire and friction at the free end. The measured strain rates are up to several thousand per second. Note that since the strains vary at high frequencies the strain rates also varies; the peak values of strain rate are used.

Fig. 7 shows the longitudinal vibrations, measured and calculated at room temperature with a pulse current of 7.75 kA. Single pulses were used for these measurements to keep the wire near room temperature. Once the wire becomes hot, the temperature varies widely along the length of the wire, making it far more difficult to model the longitudinal measurements.

4. Strength

The strength of the tantalum and tungsten wires was assessed by increasing the stress in the wire at a particular temperature until it deformed or broke. The pulse amplitude of the current in the wire was increased in small steps at a particular temperature (the current pulse frequency being carefully reduced). The current was kept constant for 3–5 min before taking the next step increase. This was continued until the wire started to bend or kink at the hottest spot, roughly halfway between the supports.

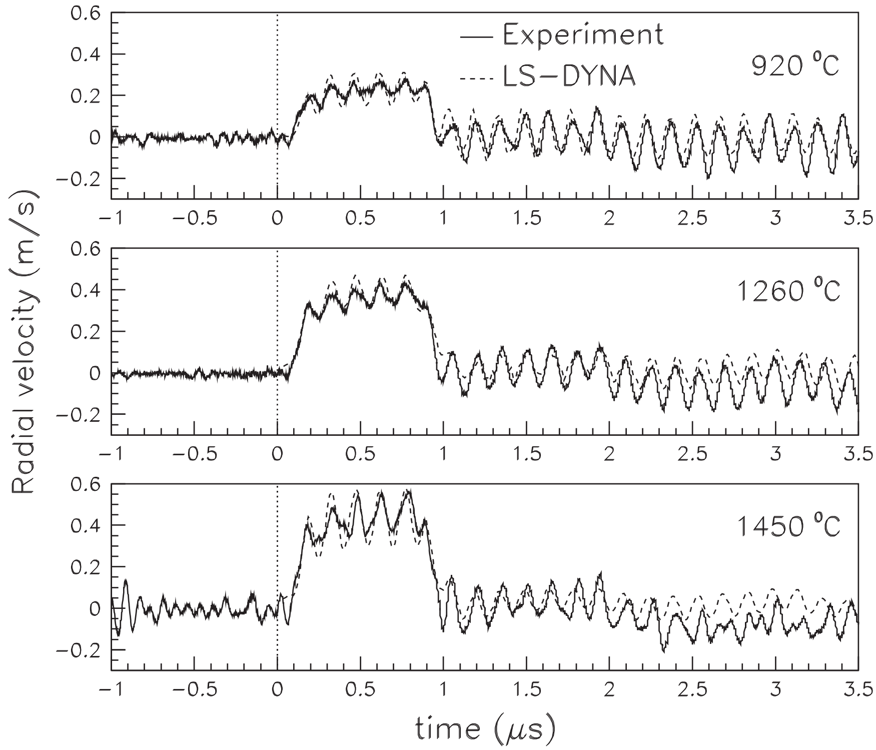

Fig. 6. Measured and calculated radial velocity of a 0.5 mm diameter tungsten wire at peak temperatures of 920, 1260 and 1450 °C.

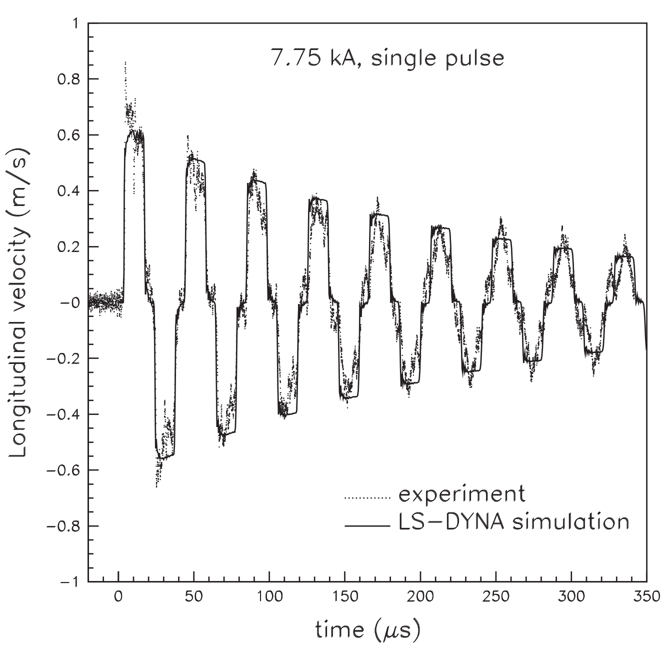

Fig. 7. Longitudinal velocity measurement and LS-DYNA modelling. Single pulse mode at 7.75 kA pulse current and the wire close to room temperature.

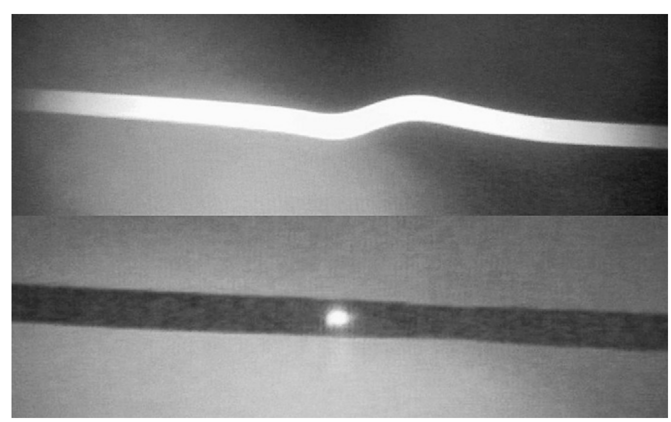

Fig. 8. Two tungsten wires, 0.5 mm diameter, about to fail in bending (top picture, hot wire) and stretching (bottom picture, cold wire showing the laser spot from the vibrometer on the wire).

Occasionally the wire would thin and break; these failure modes are shown in Fig. 8 for a tungsten wire. In addition, it was noticed that the vibrometer radial velocity signal would become very noisy as one approached the first signs of failure, eventually resulting in the loss of any coherent vibration signal.

Once a wire has begun to distort under high stress, it has been demonstrated [29] by LS-DYNA calculations that the stress in the wire increases due to the curvature of the wire, as shown in Fig. 9. Also accompanying the bending, there is usually stretching and thinning of the wire at the hottest point, so the stress and temperature of the wire increases locally. This all happens within a few pulses and is soon followed by failure, so that it is difficult to measure the temperature, diameter and hence the true stress in the wire as it is failing. However, the values of both temperature and stress are conservative (on the low side) as they represent the measurements immediately before failure.

Fig. 10 shows a plot of the stress at which a tantalum wire failed as a function of temperature. The lower edge of the wide band indicates the stress at which the wire still appeared undamaged and the upper edge the stress at which the wire started to fail. This broad line indicates the yield stress of the tantalum under the dynamic conditions of stress applied to the wire. Clearly it is not a precise point but is dependant on the number of cycles at a particular stress. The upper edge of the band indicates failure after only a few cycles; but this is superimposed on the previous history. Bands are shown for wires of 0.5 and 0.8 mm diameter. The results were repeatable to within $\pm 5\%$ of the stress. The pulsed temperature was not easy to

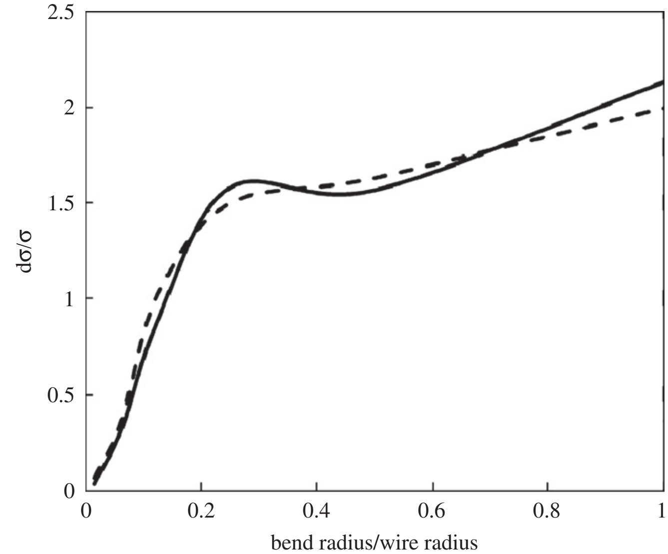

Fig. 9. Fractional increase in stress $d\sigma/\sigma$ in a straight wire as it bends, where σ is the stress in the straight wire, as a function of the bend radius/wire radius (from reference [29]). The solid line is for the increase in surface stress at the outside of the bend radius and the dotted for the inside of the bend radius.

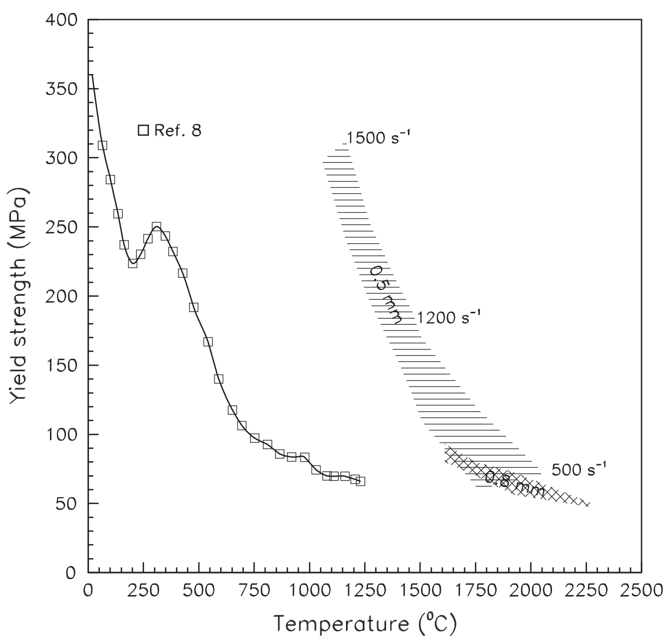

Fig. 10. Measured ultimate yield strength versus peak temperature for tantalum wires of 0.5 and 0.8 mm diameter. The strain rate is given at various points along the curve. Also shown are results from the literature [8] at low strain rates of 0.0015 and 0.00015 s^{-1}.

measure accurately with the optical pyrometer due to the temperature fluctuating with the current pulse, but was estimated to be within ± 25 K. Also shown are data from the literature [8].

Fig. 11 shows a similar plot for tungsten wires of 0.5 mm diameter. The dotted lines are the measured yield strengths taken from the literature [30] for radiated and un-irradiated tungsten. Also shown are literature data from measurements [31] taken at temperatures up to 5000 F (2760 °C). Both sets of literature data were measured at very low strain rates. The new measurements at high strain rate indicate a considerably higher yield strength than those measured at low strain rate over the entire measured temperature range, as might be expected.

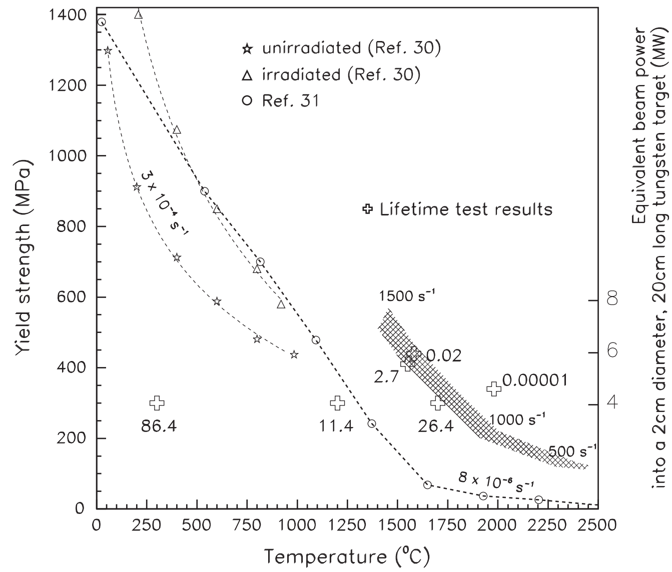

Fig. 11. Ultimate yield strength and lifetime of tungsten wires of 0.5 mm diameter versus peak temperature. The upper edge of the band indicates the stress at which the wire deformed or broke after a few pulses and the lower edge indicates where the wire was not deformed. The stress corresponding to the beam power hitting a 2 cm diameter target is shown on the right hand side axis. The strain rate is indicated at various points along the curve. The lifetime, in millions of pulses, is shown against the open crosses. Also shown are measured values of yield strength taken at very low strain rates from Ref. [30] (for irradiated and un-irradiated tungsten) and from Ref. [31].

Table 1
Results of tungsten wire lifetime tests. The "Beam Power" columns show the equivalent beam power for a full size target of 2(3) cm diameter for the same stress in the test wire. Assumes a parabolic beam distribution, 3 micro-pulses per macro-pulse of ~20 μs and beam diameter equal to target diameter. The lifetime of a target is shown in the last column, assuming 1 year of operation is 26×10^6 s. With 500 circulating targets this corresponds to 2.6×10^6 pulses per target per year. The asterisk denotes the same wire operated initially at 5840 A for 9×10^6 pulses and then at 6200 A for 10.1×10^6 pulses.

Current (A)	Temperature (K)	No. of pulses (millions)	Beam power (MW)	Target lifetime (years)
5560	1900	4.2	2.7(5.0)	1.6
5840*	2050	> 9.0	3.0(5.4)	> 3.5
6200*	2000	10.1	3.3(6.1)	3.9
6520	1940	26.4	4.1(8.7)	10.2
4720	1840	> 54.4	2.1(4.5)	> 20.9
6480	~600	> 80.8	4.0(8.6)	> 31.1
6480	1480	> 11.4	4.0(8.6)	> 4.4

The strain rates for the measurements of both tantalum and tungsten cover the range 500–1500 s^{-1}; the strain rates decrease at high temperatures. The strain rates for the Neutrino Factory target are in the range 500–1000 s^{-1} so the results for the wire are applicable to the target.

5. Lifetime

Table 1 shows a few results of tests where wires were pulsed until they broke (or the run was terminated) at fixed pulse currents (i.e., stress, or equivalent beam power in a full sized 2 cm diameter target) and peak temperatures. The repetition rate of the power supply is adjusted to give the desired wire temperature at any current. Tantalum had a relatively short life and was rapidly abandoned in favour of tungsten. The table shows the pulse current, the peak operating temperature and the number of pulses run or at failure. The next to last column shows the equivalent beam power in a target of 2 cm diameter and, in brackets, the power in a target of 3 cm diameter.

Since it is proposed to operate with ~500 targets, each target will enter the beam every 10 s. Hence a target will receive 10^6 pulses in 10^7 s of operation, or one third of a year. The last column of Table 1 gives the equivalent life of a target in the Neutrino Factory (500 circulating targets and the machine operates for 26 million seconds (300 days) per year). The tests show that targets can be expected to have lives of several tens of millions of pulse, equivalent to 10 years, so it is reasonable to assume a life of at least 3 years before changing the targets.

The lifetime is sometimes shortened in the tests when the tungsten wire reacts with the graphite jaws to form hard protuberances of tungsten carbide, resulting in the premature failure of the wire due to seizure in the jaws at the free end. Alternatively, the jaws would wear causing poor electrical conduct and overheating at the free end, again causing the wire to fail.

The lifetime measurements are also shown in Fig. 11. The long lifetimes fall below the broad line representing the failure stress, as would be expected. A few points are very close to the failure band and have lives of millions of pulses; however, once over the lower limit of the band the life falls drastically. It would appear that the stress/temperature line between long and short life is fairly well defined. Confidence has been built up such that the targets will last almost indefinitely provided the operational point is below the broad strength band. The observed failures of the wire at stresses below this strength band are almost certainly due to the wire sticking in the carbon jaws or poor electrical connections in the jaws causing overheating.

6. Electron microscope examination[2]

Some of the failed wires were sectioned near a break or at a point where the wire had thinned or buckled, and examined under a scanning electron microscope for signs of stress failure, but no direct evidence of this was found in any of the samples. Where the wire had broken the next current pulse caused sparking and melting at the break so that any evidence of stress cracking was obliterated. Generally the results were somewhat inconclusive.

7. Conclusions

It has been shown that the modelling of surface vibrations of the wires agrees very well with the measurements. This will allow the calculation of the stresses of more complicated shapes of practical targets to be performed with confidence.

It is believed that the yield strength of tungsten and tantalum has been measured under dynamic conditions at higher temperatures than previously recorded in the literature.

The lifetime of tungsten wires has been shown to be several years under the stresses to be found in a Neutrino Factory target. Although the optimum pion yield is for a target of ~1 cm in diameter, it is proposed to be conservative and operate with 2 cm diameter tungsten targets at a temperature of 1200 °C. Fig. 11 indicates that the peak stress in the tungsten target at this temperature is well below the yield strength of the material. This should allow a life of at least 3 years between replacements of the targets.

Fig. 11 shows that the target could operate reliably at beam powers approaching 8 MW at 1200 °C. Alternatively, the target diameter could be reduced to ~1.5 cm to increase the pion yield. However, to improve the margin of safety it would then be advisable to increase the number of target bars to lower the peak temperature to ~1000 °C.

Acknowledgements

J.R.J. B. and G.P. S. would like to thank members of the ISIS management and the Pulsed Power Section of the Electrical Engineering Group of ISIS for their unstinting support and generosity in giving access to the spare pulsed power supply and general help with the experiments.

References

[1] See the proceedings of NuFact from 1999 to 2006, e.g. NuFact05; Nucl. Phys. B 155 (2006) (Proc. Suppl.).
[2] J. Strait, N.V. Mokhov, S.I. Striganov, Phys. Rev. Spec. Top. Accel. Beams 13 (2010) 111001.
[3] J. Back, Presentation at UKNF meeting, 4 April 2008, 〈http://hepunx.rl.ac.uk/uknf/wp3/pimuyields/piMuYield_UKNF_Apr08.pdf〉.
[4] S. Brooks, Muon Capture Schemes for the Neutrino Factory, D. Phil. Thesis, Trinity College, Oxford, 2010. http://ora.ouls.ox.ac.uk/objects/uuid:7b724028-e4ef-4248-9d42-505e571c9e19.
[5] N.V. Mokhov, Report No. Fermilab-FN-628, 1995; N.V. Mokhov, S. I. Striganov (Eds.), in: Proceedings of the Hadronic Shower Simulation Workshop, Fermilab, 2006, AIP Conference Proceedings No. 896 (AIP, New York, 2007), pp. 50–60 〈http://www-ap.fnal.gov/MARS/〉.
[6] J. Chen, G.S. Bauer, T.A. Broome, F. Carsughi, Y. Dai, S.A. Malloy, M. Roedig, W.F. Sommer, H. Ullmaier, J. Nucl. Mater. 318 (2003) 56.
[7] D.J.S. Findlay, ISIS, pulsed neutron and muon source, in: Proceedings of Particle Accelerator Conference 07, Albuquerque, New Mexico, USA, p. 695, 2007.
[8] J.W. Pugh, Trans. Am. Soc. Met. 48 (1956) 677.
[9] E. Lasner, W.-D. Schubert, Tungsten, Kluwer Academic/Plenum Publishers, New York, 1999.
[10] C.D. Johnson, NuFact99, Lyon, 〈http://lyoinfo.in2p3.fr/nufact99/agenda/html〉.
[11] MERIT Home Page, 〈http://proj-hiptarget.web.cern.ch/proj-hiptarget/default.asp?meet=true〉.
[12] B.J. King, S.S. Moser, R.J. Weggel, N.V. Mokhov, in: Proceedings of the IEEE Particle Accelerator Conference, New York City, NY, USA, IEEE 99Ch36366, 29 March–2 April, 1999, p. 3041.
[13] S. O'Day, F. Bieniosek, K. Anderson, 0-7803.1203-l/93$03.00 0 1993, IEEE Particle Accelerator Conference, 1993, p. 3096, 〈http://epaper.kek.jp/p93/PDF/PAC1993_3096.PDF〉.
[14] P. Hurh, 〈http://www-mhf.desy.de/public/care04/2004.11.03_sr2/target_bene_hurh.pdf〉.
[15] R.W. Armstrong, S.M. Walley, Int. Mater. Rev. 53 (2008) 105.
[16] C.J. Densham, O. Caretta, P. Loveridge, T.W. Davies, R. Woods, The Potential of Fluidised Powder Target Technology in High Power Accelerator Facilities, Particle Accelerator Conference, 09, Vancouver, BC, Canada, 2009, 〈http://trshare.triumf.ca/~pac09proc/Proceedings/〉.
[17] J.R.J. Bennett, Nucl. Instr. and Meth. A 451 (2000) 344.
[18] J.R.J. Bennett, AIP Conf. Proc. 542 (2000) 253.
[19] J.R.J. Bennett, C.N. Booth, R.A. Brownsword, C.J. Densham, T.R. Edgecock, A.J. McFarland, G.P. Skoro, Nucl. Phys. B (Proc. Suppl.) 155 (2006) 291.
[20] J.R.J. Bennett, C.N. Booth, R.A. Brownsword, C.J. Densham, T.R. Edgecock, G.P. Skoro, Nucl. Phys. B (Proc. Suppl.) 155 (2006) 293.
[21] J.R.J. Bennett, Nucl. Instr. and Meth. A 562 (2006) 924.
[22] J.R.J. Bennett, G.P. Skoro, C.N. Booth, S.J. Brooks, R.A. Brownsword, T.R. Edgecock, C.J. Densham, S.A. Gray, A.J. McFarland, N. Simos, D. Wilkins, J. Nucl. Mater. 377 (2008) 285.
[23] Polytec web site, 〈http://www.polytec.com〉.
[24] G.P. Škoro, J.R.J. Bennett, T.R. Edgecock, S.A. Gray, A.J. McFarland, C.N. Booth, K.J. Rodgers, J.J. Back, J. Nucl. Mater. 409 (2010) 40.
[25] Livermore Software Technology Corp. 〈http://www.lstc.com/〉.
[26] J. Crank, The Mathematics of Diffusion, 2nd ed., Oxford University Press, 1975.
[27] J.W. Davis, ITER Material Properties Handbook, 1997.
[28] AFCI Materials Handbook, LA-CP-06-0904 (Revision 5), 2006.
[29] G.P. Skoro, Violin Modes in Tungsten Wires, UKNF meeting, RAL, 25 April 2007, 〈http://hepunx.rl.ac.uk/uknf/wp3/wiretest/sims/Tungsten/Violin_modes_in_tungsten_wire.ppt〉.
[30] J.M. Steichen, J. Nucl. Mater. 60 (1976) 13.
[31] C.A. Drury, R.C. Kay, A. Bennett, A.J. Albom, Mechanical Properties of Wrought Tungsten, ASD-TDR-63-585, Vol. II, 1963.

[2] Performed by BegbrokeNano, Begbroke Science Park, Sandy Lane, Yarnton, Oxford, OX5 1PF. http://begbrokenano.materials.ox.ac.uk/